PERMANENT MAGNET SYNCHRONOUS MOTOR DRIVE SYSTEM FOR MECHATRONICS APPLICATIONS

Adel El Shahat[1,*] & Hamed El Shewy[2]

[1] Mechatronics-Green Energy Lab., Electrical & Computer Engineering Dept., Ohio State University, USA
[2] Department of Electrical Power and Machines Engineering, Zagazig University, Egypt
[*] E-mail: adel.elshahat@ieee.org , ahmed.210@osu.edu, adel2029@yahoo.com

ABSTRACT

In this paper, a field oriented controlled PM motor drive system is described and analyzed due to its importance in many applications especially in mechatronics applications. Permanent Magnet Synchronous Motors (PMSM) are widely applied in industrial and robotic applications due to their high efficiency, low inertia and high torque – to – volume ratio. A closed loop control system with a PI controller in the speed loop has been designed to operate in constant torque angle and flux weakening regions. A comparative study of hysteresis and PWM control schemes associated with current controllers has been made. Then, the simulation of a field oriented controlled PM motor drive system is developed using Simulink. The simulation circuits for PM synchronous motor, inverter, speed and current controllers include all realistic components of the drive system. Simulation results for both hysteresis and PWM control schemes associated with current controllers are given for two speeds of operation, one below rated and another above rated speed.

Keywords: *Permanent Magnet, Synchronous Motor, Field Oriented, Control, Simulink, Drive, PI Controller, Torque Angle, Flux Weakening, Hysteresis, PWM.*

1. INTRODUCTION

Among the ac drives, permanent magnet synchronous machine (PMSM) drives have been increasingly applied in a wide variety of industrial applications and mechatronics applications. The reason comes from the advantages of PMSM: high power density and efficiency, high torque to inertia ratio, and high reliability. Recently, the continuous cost reduction of magnetic materials with high energy density and coercitivity (e.g., samarium cobalt and neodymium-boron iron) makes the ac drives based on PMSM more attractive and competitive. In the high performance applications, the PMSM drives are ready to meet sophisticated requirements such as fast dynamic response, high power factor and wide operating speed range. Consequently, a continuous increase in the use of PMSM drives will surely be witnessed in the near future [1-3]. The vector control (or called field-oriented control) of ac machines was introduced in the late 1960s by Blaschke, Hasse, and Leonhard in Germany. Following their pioneering work, this technique, allowing for the quick torque response of ac machines similar to that of dc machines, has achieved a high degree of maturity and become popular in a broad variety of applications. It is also widely applied in many areas where servo-like high performance plays a secondary role to reliability and energy savings. To achieve the field-oriented control of PMSM, knowledge of the rotor position is required. Usually the rotor position is measured by a shaft encoder, resolver, or Hall sensors. [4-8]. The advantages of PM machines recently make them highly attractive candidates for "direct drive" applications, such as hybrid electrical vehicles (HEV) or electrical vehicles (EV) [11- 16] and washing machines, which are illustrated in Figure 1. By this technology, the rotating working unit of a direct drive system, such as the basket or drum of a washing machine, is coupled to the motor shaft without transmission assembly, which may include clutches, belts, pulleys and/or gearboxes. The power is directly delivered to the working unit by the motor. The concept of direct drive enables the high dynamic response, increased efficiency, low acoustic noise, and long lifetime due to the elimination of the transmission components. Such direct drive systems normally require large shaft torque at standstill (i.e., zero speed) and low speeds as well as constant output power over wide speed range. In order to meet such requirements, the PM machines are designed to operate not only in the constant torque mode when their speed is below the base (or rated) speed but also in the constant power mode when above the base speed. In this way, the cost and size of overall drive system can be significantly reduced. The constant torque operation of PM motor can be easily achieved by conventional vector control. However, when the speed is above the base speed, the back-EMF of PM motor is larger than the line voltage and then the motor suffers from the difficulty to continuously produce torque due to voltage and current constraints. Thanks to the flux-weakening technology, the operating speed range can be extended by applying negative magnetizing current component to weaken the air-gap flux [9, 10]. transform are in widespread use.

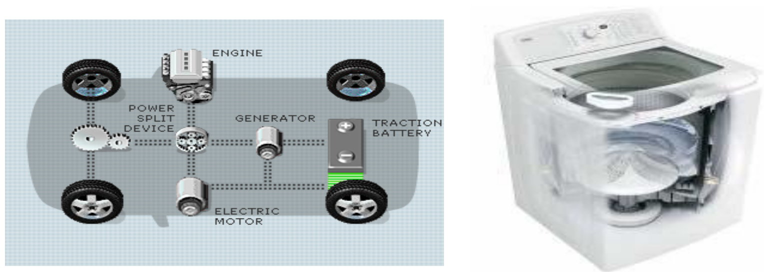

(a) **(b)**

Figure 1. Applications of PMSM Drive System; (a) HEV, (b) Washing Machine

2. DESCRIPTION OF DRIVE SYSTEM

This section deals with the description of the drive system which includes different components such as permanent magnet motors, position sensors, inverters and current controllers. The motor drive consists of four main components, the PM motor, inverter, control unit and the position sensor. The components are connected as shown in figure 2.

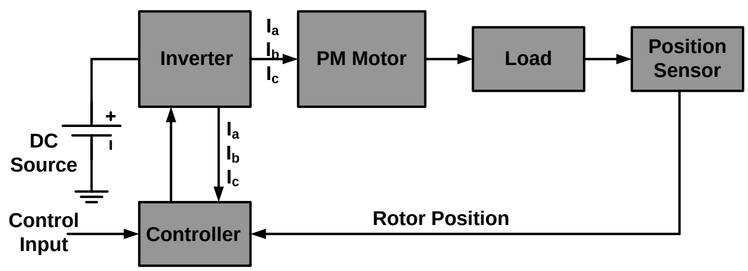

Figure 2. Drive System Schematic

2.1. Current Controlled Inverter

The motor is fed form a voltage source inverter with current control. The control is performed by regulating the flow of current through the stator of the motor. Current controllers are used to generate gate signals for the inverter. Proper selection of the inverter devices and selection of the control technique will guarantee the efficacy of the drive. Voltage Source Inverters are devices that convert a DC voltage to AC voltage of variable frequency and magnitude. They are very commonly used in adjustable speed drives and are characterized by a well defined switched voltage wave form in the terminals [17]. Both current source inverters (CSI) and voltage source inverters (VSI) can be operated in controlled current modes. The current source inverter is a "natural" current supply and can readily be adapted to controlled current operation. The voltage source inverter requires more complexity in the current regulator but offers much higher bandwidth and elimination of current harmonics as compared to the CSI and is almost exclusively used for motion control applications. Current controllers can be classified into two groups, hysteresis and PWM current controllers. Both types are discussed below.

2.1.1. Hysteresis current controller

Hysteresis current controller can also be implemented to control the inverter currents. The controller will generate the reference currents with the inverter within a range which is fixed by the width of the band gap. In this controller the desired current of a given phase is summed with the negative of the measured current. The error is fed to a comparator having a hysteresis band. When the error crosses the lower limit of the hysteresis band, the upper switch of the inverter leg is turned on. But when the current attempts to become less than the upper reference band, the bottom switch is turned on. Fig. 3 shows the hysteresis band with the actual current and the resulting gate signals. This controller does not have a specific switching frequency and changes continuously but it is related with the band width [17] [18].

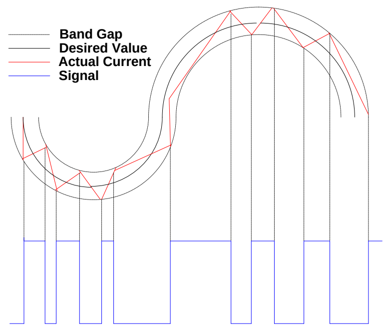

Figure 3. Hysteresis controller

2.1.2. PWM Current Controller

PWM current controllers are widely used. The switching frequency is usually kept constant. They are based in the principle of comparing a triangular carrier wave of desire switching frequency with error of the controlled signal. The error signal comes from the sum of the reference signal generated in the controller and the negative of the actual motor current. The comparison will result in a voltage control signal that goes to the gates of the voltage source inverter to generate the desire output. Its control will respond according to the error. If the error command is greater than the triangle waveform, the inverter leg is held switched to the positive polarity (upper switch on). When the error command is less than the triangle waveform, the inverter leg is switched to the negative polarity (lower switch on). This will generate a PWM signal like in fig. 4. The inverter leg is forced to switch at the frequency of the triangle wave and produces an output voltage proportional to the current error command. The nature of the controlled output current consists of a reproduction of the reference current with high-frequency PWM ripple superimposed [17].

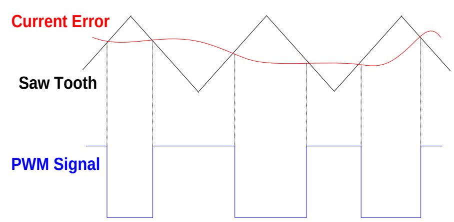

Figure 4. PWM current controller

2.2. Field Oriented Control of PM Motors

The PMSM control is equivalent to that of the dc motor by a decoupling control known as field oriented control or vector control. The vector control separates the torque component of current and flux channels in the motor through its stator excitation. The vector control of the PM synchronous motor is derived from its dynamic model. Considering the currents as inputs, the three currents are:

$$\begin{aligned} i_a &= I_s \sin(\omega_r t + \alpha) \\ i_b &= I_s \sin(\omega_r t + \alpha - \frac{2\pi}{3}) \\ i_c &= I_s \sin(\omega_r t + \alpha + \frac{2\pi}{3}) \end{aligned} \quad (1)$$

where α is the angle between the rotor field and stator current phasor, ω_r is the electrical rotor speed. The previous currents obtained are the stator currents that must be transformed to the rotor reference frame with the rotor speed ω_r, using Park's transformation. The q and d axis currents are constants in the rotor reference frames since α is a constant for a given load torque. As these constants, they are similar to the armature and field currents in the separately excited dc machine. The q axis current is distinctly equivalent to the armature current of the dc machine; the d axis current is field current, but not in its entirety. It is only a partial field current; the other part is contributed by the equivalent current source representing the permanent magnet field. For this reason the q axis current is called the torque producing component of the stator current and the d axis current is called the flux producing component of the stator current. i_d and i_q in terms of I_s as follows:

$$\begin{pmatrix} i_q \\ i_d \end{pmatrix} = I_s \begin{pmatrix} \sin\alpha \\ \cos\alpha \end{pmatrix} \quad (2)$$

The electromagnetic torque equation is obtained as given below.

$$T_e = \frac{3}{2}\frac{P}{2}[\frac{1}{2}(L_d - L_q)I_s^2 \sin 2\alpha + \lambda_{af} I_s \sin\alpha] \quad (3)$$

2.2.1. Constant Torque Operation

Constant torque control strategy is derived from field oriented control, where the maximum possible torque is desired at all times like the dc motor. This is performed by making the torque producing current i_q equal to the supply current I_s. That results in selecting the α angle to be 90º. By making the i_d current equal to zero the torque equation can be rewritten as:

$$T_e = (\frac{3}{2})(\frac{P}{2})\lambda_{af} I_q \quad (4)$$

Assuming that:

$$k_t = (\frac{3}{2})(\frac{P}{2})\lambda_{af} \quad (5)$$

The torque is give by

$$T_e = k_t . I_q \quad (6)$$

Like the dc motor, the torque is dependent of the motor current.

2.2.2. Flux-weakening

Flux weakening is the process of reducing the flux in the d axis direction of the motor which results in an increased speed range. The motor drive is operated with rated flux linkages up to a speed where the ratio between the induced emf and stator frequency (V/f) is maintained constant. After the base frequency, the V/f ratio is reduced due to the limit of the inverter dc voltage source which is fixed. The weakening of the field flux is required for operation above the base frequency. This reduces the V/f ratio. This operation results in a reduction of the torque proportional to a change in the frequency and the motor operates in the constant power region [19]. The rotor flux of PMSM is generated by permanent magnet which can not be directly reduced as induction motor. The principle of flux-weakening control of PMSM is to increase negative direct axis current and use armature reaction to reduce air gap flux, which equivalently reduces flux and achieves the purpose of flux-weakening control [20]. This method changes torque by altering the angle between the stator MMF and the rotor d axis. In the flux weakening region where $\omega_r > \omega_{rated}$ angle α is controlled by proper control of id and i_q for the same value of stator current. Since i_q is reduced the output torque is also reduced. The angle α can be obtained as:

$$\alpha = \tan^{-1}(\frac{i_q}{i_d}) \quad (7)$$

The current I_s is related to i_d and i_q by:

$$I_s = \sqrt{(i_d^2 + i_q^2)} \quad (8)$$

Using α and rotor position the controller will generate the reference currents; then the current controller makes uses of the reference signals to control the inverter for the desired output currents. The load torque is adjusted to the maximum available torque for the reference speed:

$$T_L = T_{e(rated)}(\frac{\omega_{rated}}{\omega_r}) \quad (9)$$

2.3. Implementation of the Speed Control Loop of PM Motor

Many applications, such as robotics and factory automation, require precise control of speed and position. Speed Control Systems allow one to easily set and adjust the speed of a motor. The control system consists of a speed feedback system, a motor, an inverter, a controller and a speed setting device. A properly designed feedback controller makes the system insensible to disturbance and changes of the parameters. The purpose of a motor speed controller is to take a signal representing the demanded speed, and to drive a motor at that speed. Closed Loop speed control systems have fast response, but become expensive due to the need of feed back components such as speed sensors. For a PM motor drive system with a full speed range the system will consist of a motor, an inverter, a controller (constant torque and flux weakening operation, generation of reference currents and PI controller) as shown in fig. 5.

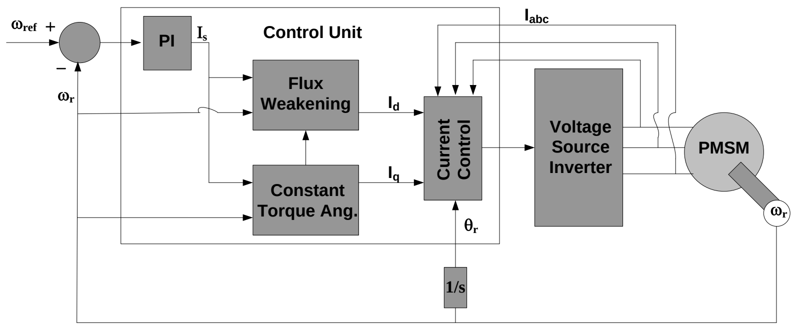

Figure 5. Drive Block Diagram

The operation of the controller must be done according to the speed range. For operation up to rated speed it will operate in constant torque region and for speeds above rated speed it will operate in flux-weakening region. In this region the d-axis flux and the developed torque are reduced. The process can be easily understood with the flow diagram in fig. 6.

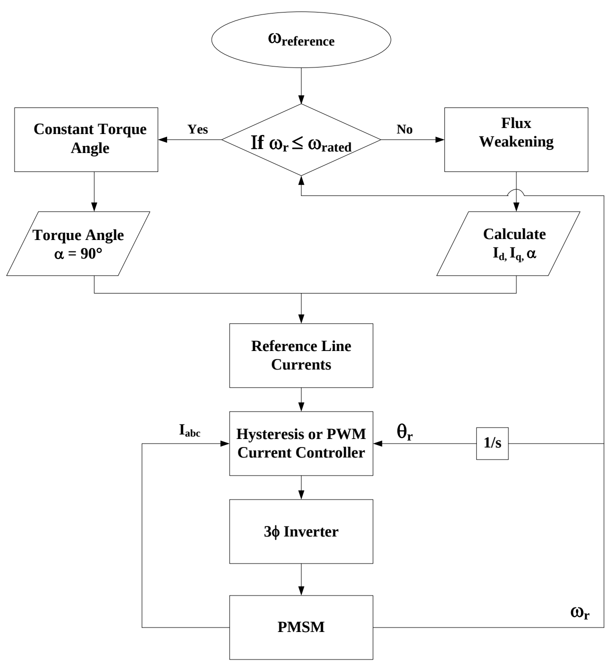

Figure 6. System Flow Diagram

Speed controller calculates the difference between the reference speed and the actual speed producing an error, which is fed to the PI controller. PI controllers are used widely for motion control systems. They consist of a proportional gain that produces an output proportional to the input error and an integration to make the steady state error zero for a step change in the input. Block diagram of the PI controller is shown in fig. 7.

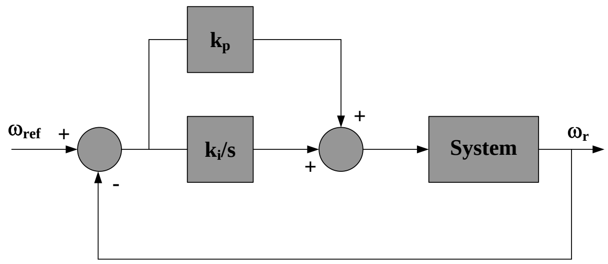

Figure 7. PI Controller

Speed control of motors mainly consist of two loops the inner loop for current and the outer loop for speed. The order of the loops is due to their response, how fast they can be changed. This requires a current loop at least 10 times faster than the speed loop. Since the PMSM is operated using field oriented control, it can be modeled like a dc motor. The design begins with the innermost current loop by drawing the block diagram. But in PMSM drive system the motor has current controllers which make the current loop. The current control is performed by the comparison of the reference currents with the actual motor currents. The design of the speed loop assumes that the current loop is at least 10 times faster than speed loop, allowing reducing the system block diagram by considering the current loop to be of unity gain as shown in fig. 8.

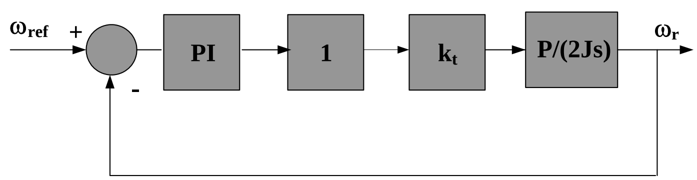

Figure 8. Block Diagram of Speed Loop

For our SPMSM; k_t = (3/2) (P/2) λ_{af} = 0.849; where: λ_{af} = 0.283; P = 4; J = 0.0000144 The open loop transfer function of the motor is given by:

$$GH(s) = (k_i / s + k_p)(k_t)(2 / Js) \tag{10}$$

For stable system and to satisfy dynamic response without oscillations the phase margin (ϕ_{PM}) usually greater than 45º, here we prefer it to be 60º. Knowing the motor parameters and the phase margin, with the gain margin definitions the k_i and k_p gains can be obtained for the motor controller using the following equations.

$$|GH(j\omega)| = |(k_i / (j\omega) + k_p)(k_t)(2 / J(j\omega))| = 1 \tag{11}$$

For crossover frequency (selected) f_c = 100 Hz; ($\omega_c = 2\,\pi\,f_c$ = 628.3185 rad/sec)

$$\text{Angle } GH(j\omega) = \angle(k_i / (j\omega) + k_p)(k_t)(2 / J(j\omega)) = 180^\circ + \phi_{PM} \tag{12}$$

The gains for the speed controller was obtained using the motor parameters and by selecting a crossover frequency k_p = 0.004615; ki = 1.674
A simple stability check for these obtained values is done using characteristic eq. (13), in which GH(s): Open loop transfer function, G: Feed-forward transfer function, and H: Feed-back Transfer function.

$$1 + GH(s) = 0 \tag{13}$$

The poles of the characteristic equation are: - 272. 0927 ± j 351.2237; it is clear they are in left hand side of the s-plane so the system will be stable with these values.

2.4. Inverter-Motor Equivalent Circuit

Considering the equivalent circuit of the system inverter-motor as in fig. 9; the line voltages for the motor have the expression [22], [23]:

$$v_{ab}(t) = v_{an}(t) - v_{bn}(t) \tag{14}$$
$$v_{bc}(t) = v_{bn}(t) - v_{cn}(t)$$
$$v_{ca}(t) = v_{cn}(t) - v_{an}(t)$$

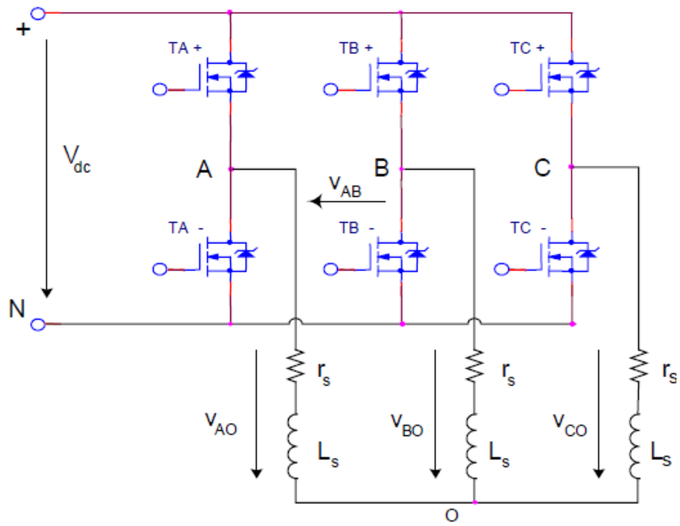

Figure 9. Inverter-motor equivalent circuit

The motor phase voltages will have the expression:

$$v_{ao}(t) = v_{an}(t) - v_{on}(t) \tag{15}$$
$$v_{bo}(t) = v_{bn}(t) - v_{on}(t)$$
$$v_{co}(t) = v_{cn}(t) - v_{on}(t)$$

Being a star connection, then at every time instant the following relation is satisfied:

$$v_{ao} + v_{bo} + v_{co}(t) = 0 \tag{16}$$

From Eq (15) and Eq (16) then the null voltage is derived as:

$$v_{on} = (v_{an} + v_{bn} + v_{cn})/3 \tag{17}$$

Having the pulses for each inverter leg (da, db, dc), the inverter's leg voltages can be found as:

$$v_{an} = V_{dc} \,.\, da \tag{18}$$
$$v_{bn} = V_{dc} \,.\, db$$
$$v_{cn} = V_{dc} \,.\, dc$$

Using the above Eq.s, the resulted line voltages will have the expression Eq (19):

$$v_{ab} = V_{dc} \,.\, (\, da - db \,) \tag{19}$$
$$v_{bc} = V_{dc} \,.\, (\, db - dc \,)$$
$$v_{ca} = V_{dc} \,.\, (\, dc - da \,)$$

Similarly, the phase voltages can be found as:

$$v_a = V_{dc} \,.\, (\, da - (da + db + dc)/3 \,) \tag{20}$$
$$v_b = V_{dc} \,.\, (\, db - (da + db + dc)/3 \,)$$
$$v_c = V_{dc} \,.\, (\, dc - (da + db + dc)/3 \,)$$

The structure of the inverter Simulink model is presented later.

2.5. Dc Source

The dc-link voltage Vdc, could be obtained using Vsn (maximum phase voltage) as follow [21]:

$$v_{dc} = \frac{2.P}{\pi}.\sin(\frac{\pi}{P}).V_{sn} \tag{21}$$

Where Vsn: peak amplitude of phase voltage

2.6. Dynamic Modeling of PMSM

Figure 10 presents equivalent circuit of PMSM in d-q axis to be used in both dynamic equations of PMSM, and static characteristics.

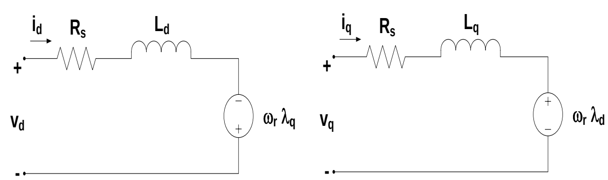

Figure 10. PMSM Equivalent Circuit

It should be notified that, all lower case symbols introduce instantaneous values, and upper case for steady state. The two axes PMSM stator windings can be considered to have equal turns per phase. The rotor flux can be assumed to be concentrated along the d axis while there is zero flux along the q axis. Further, it is assumed that the machine core losses are negligible. Also, rotor flux is assumed to be constant (variation in the rotor flux with respect to time is negligible). Variations in rotor temperature alter the magnet flux, but its variation with time is considered to be negligible. A dynamic model of PMSM can be dedicated as follow [24]:

$$v_q = r_s\, i_q + \rho(\lambda_q) + \omega_r \lambda_d \tag{22}$$

$$v_d = r_s\, i_d + \rho(\lambda_d) - \omega_r \lambda_q \tag{23}$$

$$\lambda_q = L_q i_q \tag{24}$$

$$\lambda_d = L_d\, i_d + \lambda_{af} \tag{25}$$

where ω_r : Electrical velocity of the rotor; λ_{af} : The flux linkage due to the rotor magnets linking the stator; v_d, v_q : d, q voltages; λ_d, λ_q : d, q flux; $\rho(\lambda_{af}) = 0$, $\lambda_{af} = L_m\, i_{fr}$; ρ : Derivative Operator

The electromagnetic torque is given by:

$$T_e = \frac{3}{2}\frac{P}{2}(\lambda_d i_q - \lambda_q i_d) = \frac{3}{2}\frac{P}{2}(\lambda_m i_q + (L_d - L_q) i_q i_d) \tag{26}$$

The electromechanical power

$$P_{em} = \omega_{m}\ T_e = \frac{3}{2}\omega_r\,(\lambda_d\, i_q - \lambda_q\, i_d) \tag{27}$$

$$\omega_r = \frac{P}{2}\omega_{m} \tag{28}$$

where P: Poles No; ω_{rm}: Rotor Mechanical velocity

The general mechanical equation for the motor is:

$$T_e = T_l + T_d + B\,\omega_{rm} + J\rho\,\omega_{rm} \tag{29}$$

B: Viscous frictions coefficient; J: Inertia of shaft and load system; T_d : Dry friction; T_l: Load torque

3. PMSM DRIVE SIMULATION

In this section, the simulation of a field oriented controlled PM motor drive system is developed using Simulink. The simulation circuit includes all realistic components of the drive system. A closed loop control system with a PI controller in the speed loop has been designed to operate in constant torque and flux weakening regions.

Implementation has been done in Simulink. A comparative study of hysteresis and PWM control schemes associated with current controllers has been made. Simulation results are given for two speeds of operation, one below rated and another above rated speed.

3.1. Modeling of PMSM

Modeling of a permanent magnet synchronous motor is introduced in this section using the m/c equations; with some assumptions like: Saturation is neglected; the induced EMF is sinusoidal; Eddy currents and hysteresis losses are negligible; there are no field current dynamics; all motor parameters are assumed constant; Leakage inductances are zero. Detailed modeling of PM motor drive system is required for proper simulation of the system. The d-q model has been developed on rotor reference frame. This dynamic simulation of PMSM is done with the aid of SIMULINK in MATLAB package. The voltage and load torque are considered as inputs, with the speed and current as outputs. This model is verified by the same author as in references [25], [26], [27].

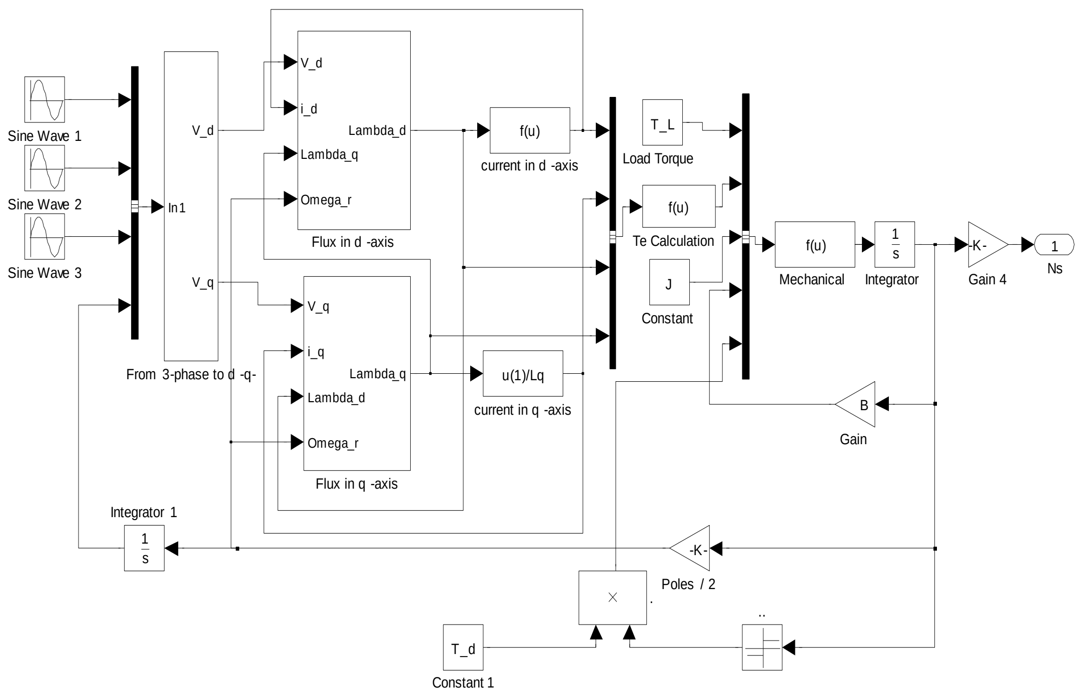

Figure 11. Permanent Magnet Synchronous Motor Model

3.2. Simulink Simulation of PMSM Drive

The PM motor drive simulation was built in several steps like abc phase transformation to dqo variables, calculation torque and speed, and control circuit. The abc phase transformation to dqo variables is built using Parks transformation and for the dqo to abc the reverse transformation is used. For simulation purpose the voltages are the inputs and the current are output. Parks transformation used for converting V_{abc} to V_{dqo} is shown in modeling and the reverse transformation for converting I_{dqo} to I_{abc} is shown in figure 12.

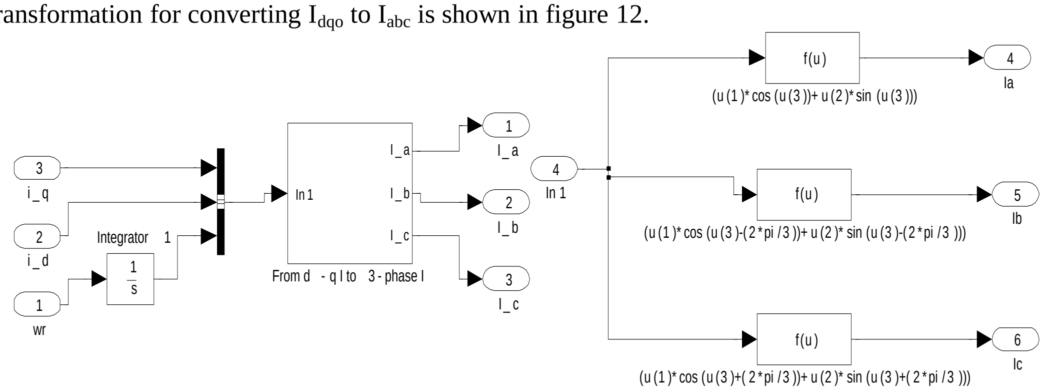

Figure 12. I_{dqo} to I_{abc} Block

The vector control requires a block for the calculation of the reference current using the α angle, the position of the rotor and the magnitude of the I_s. The block with the PI controller is shown in fig. 13.

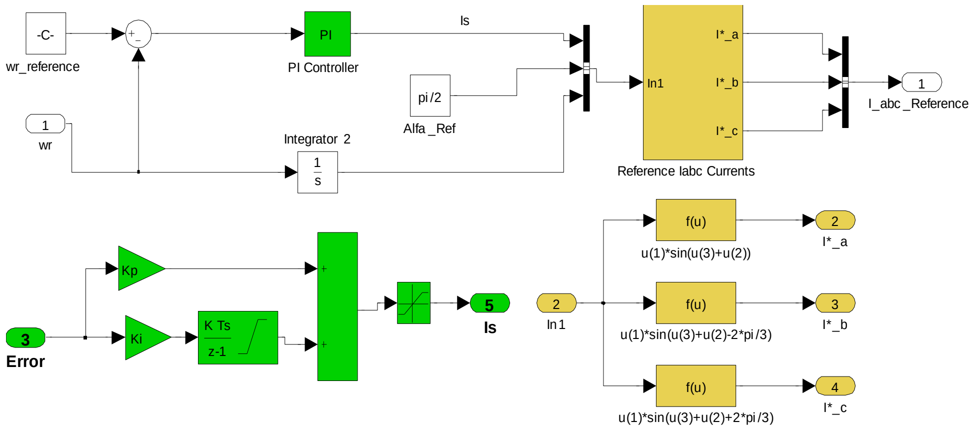

Figure 13. Vector Control Reference Current Block with PI Speed Controller

Inverter is implemented as shown in fig. 14, depending on the inverter relations introduced before.

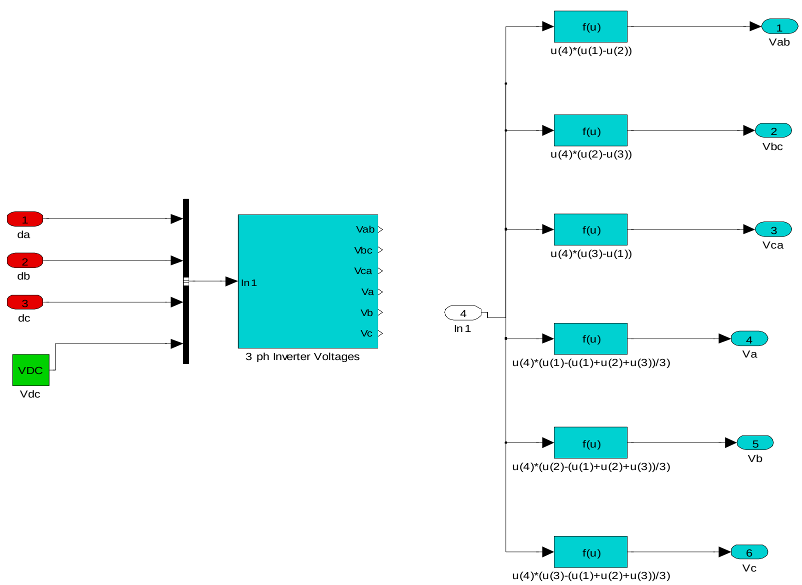

Figure 14. Voltage Source Inverter

For proper control of the inverter using the reference currents, current controllers are implemented to generate the gate pulses for the IGBT's. Current controllers used are shown in fig. 15 and 16.

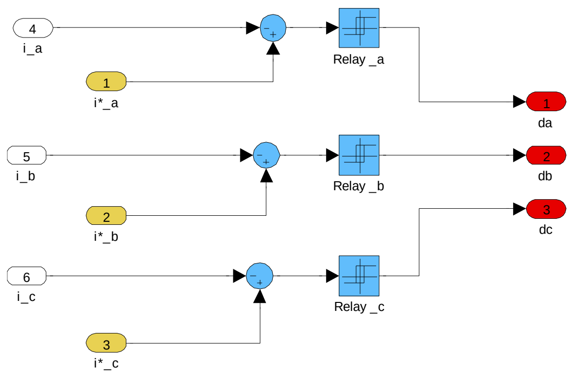

Figure 15. Hysteresis controller

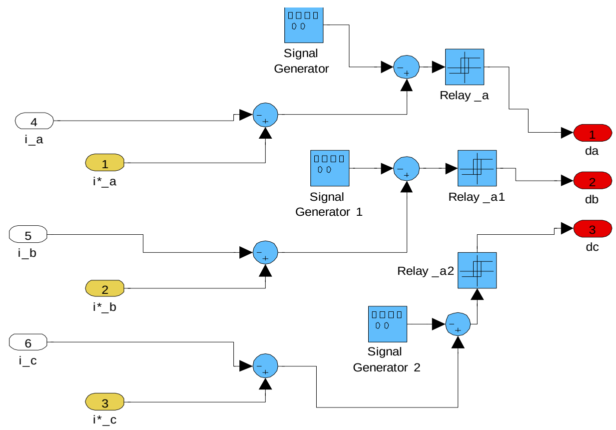

Figure16. PWM current controller

4. SIMULATION RESULTS

This part deals with the simulation results of PMSM drive system. Comparative study of the current controllers used in the system is given. The system built in Simulink for a PMSM drive system has been tested with the two current control methods, Hysteresis and PWM, at the constant torque and flux-weakening regions of operation. The motor is operated with constant torque up to its rated speed and beyond that rated speed flux-weakening mode is adopted. Simulation results are given at electrical speeds of 2000 rpm (66.6667 Hz) and 2400 (80 Hz). The above speeds represent rated and above rated speed of the motor. The simulation was carried out using two current control techniques to study the performance of the motor drive. The techniques are Hysteresis current control and PWM current control. The plots of current, torque and speed are given for both cases.

4.1. Simulation for Operation at 2000 rpm

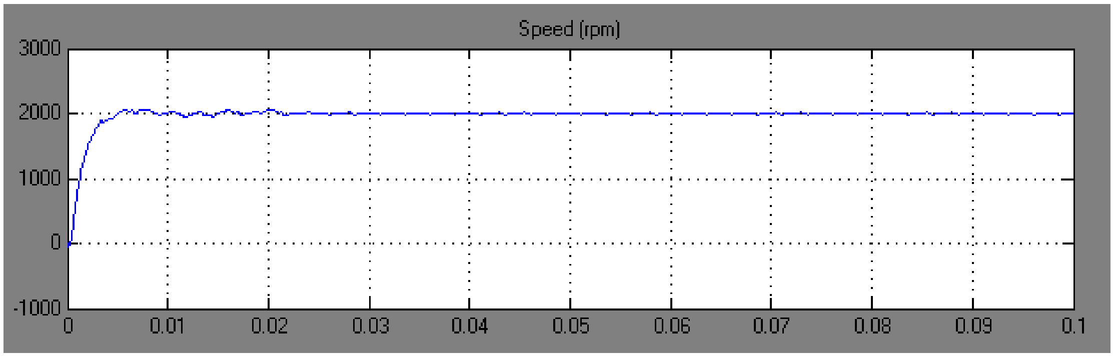

Figure 17. Electrical Speed with time (at 66.6667 Hz); for Hysteresis controller

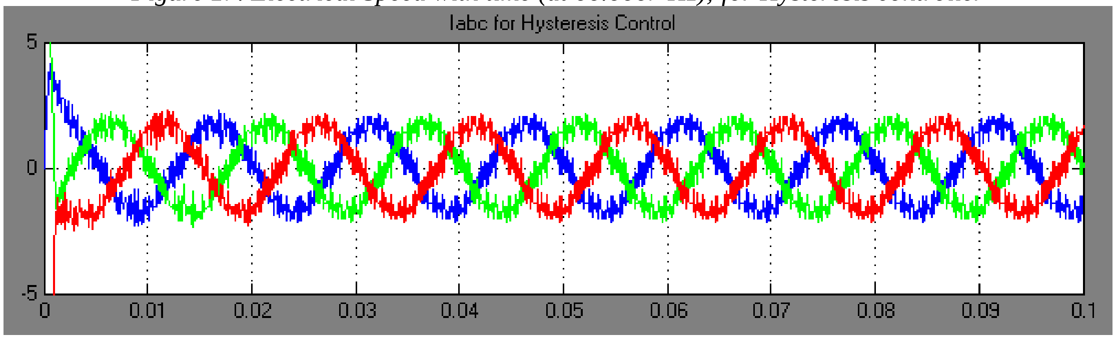

Figure 18. Iabc with time (at 66.6667 Hz); for Hysteresis controller

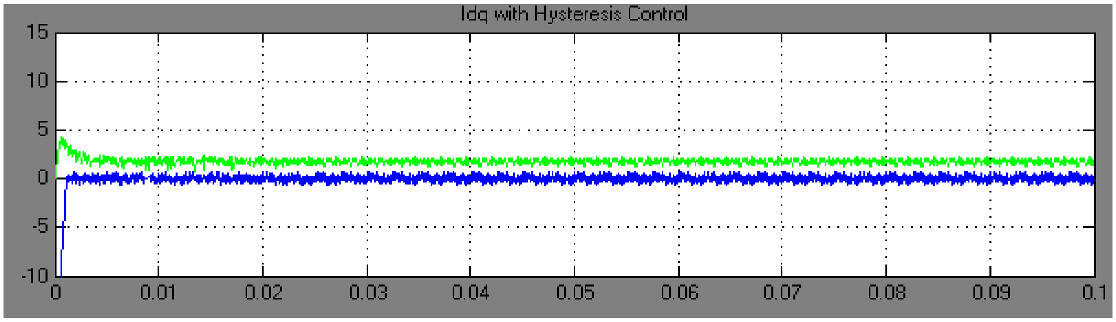

Figure 19. Idq with time (at 66.6667 Hz); for Hysteresis controller

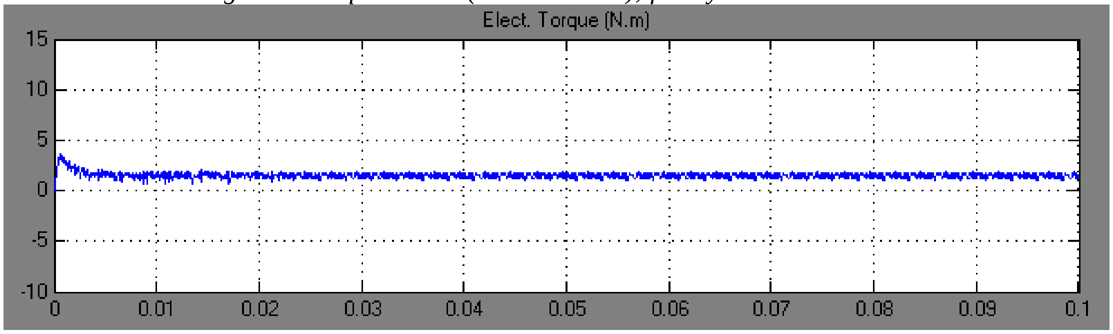

Figure 20. Torque with time (at 66.6667 Hz); for Hysteresis controller

Fig. 17 shows a variation of the speed with time. The steady state speed is the same as that of the commanded reference speed. Fig. 18 shows the three phase currents drawn by the motor as a result of the hysteresis current control. The currents are obtained using Park's reverse transformation. It is clear that the current is non sinusoidal at the starting and becomes sinusoidal when the motor reaches the controller command speed at steady state. The corresponding dq component of current is given in fig. 19 in which the value of id is zero since field oriented control is used. Fig. 20 shows the developed torque of the motor. The starting torque nearly is more than twice the steady state value. The previous plots have been repeated with PWM control for comparing with hysteresis control.

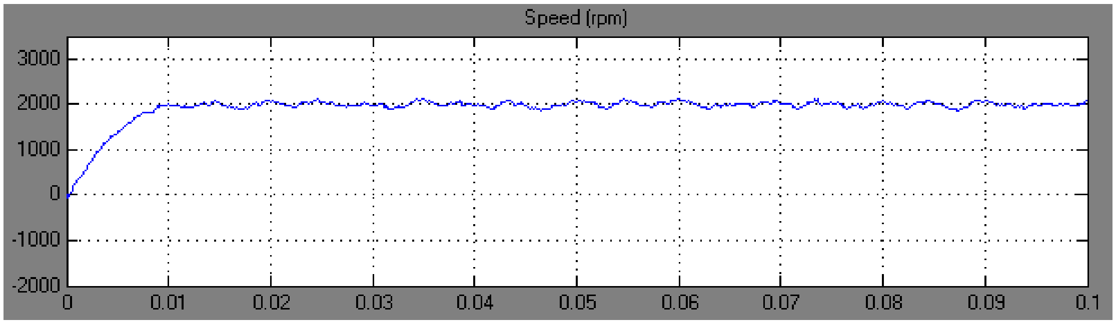

Figure 21. Electrical Speed with time (at 66.6667 Hz); for PWM controller

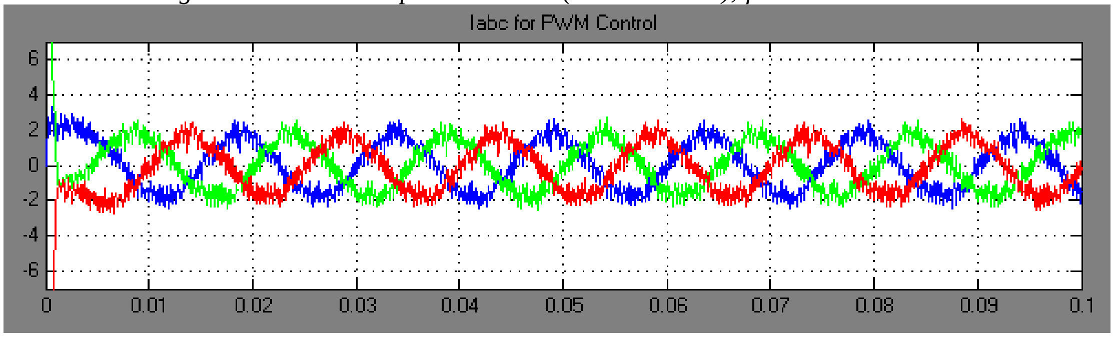

Figure 22. Iabc with time (at 66.6667 Hz); for PWM controller

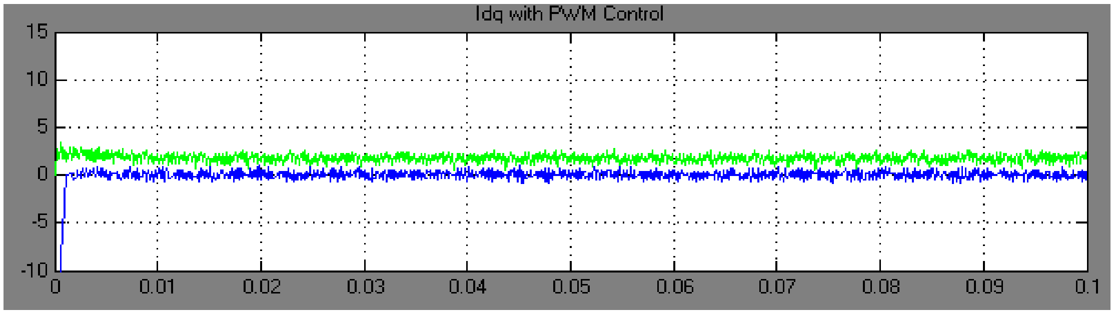

Figure 23. Idq with time (at 66.6667 Hz); for PWM controller

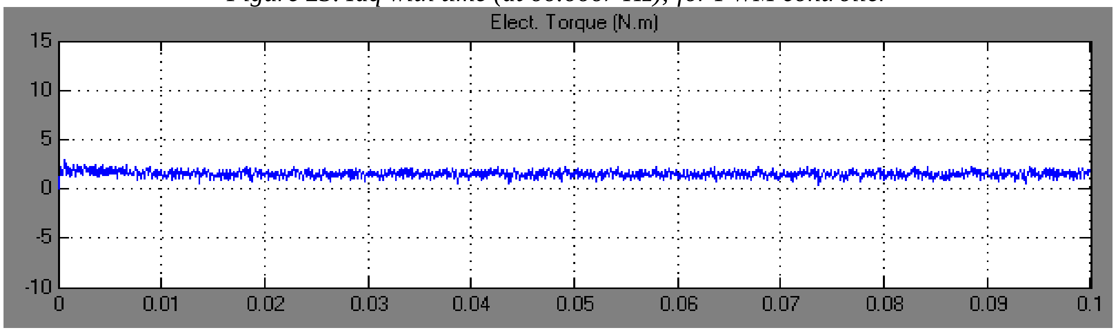

Figure 24. Torque with time (at 66.6667 Hz); for PWM controller

Fig. 21 shows a variation of the speed with time. The steady state speed is the same as that of the commanded reference speed. Fig. 22 shows the three phase currents as a result of the PWM current control obtained from Park's reverse transformation. It is clear that the current is non sinusoidal at the starting and becomes sinusoidal when the motor reaches the controller command speed at steady state. The corresponding dq component of current is given in fig. 23 with id almost equal to zero for constant torque operation. Fig. 24 shows the developed torque of the motor.

4.2. Simulation for Operation at Higher Speed of 2400 rpm

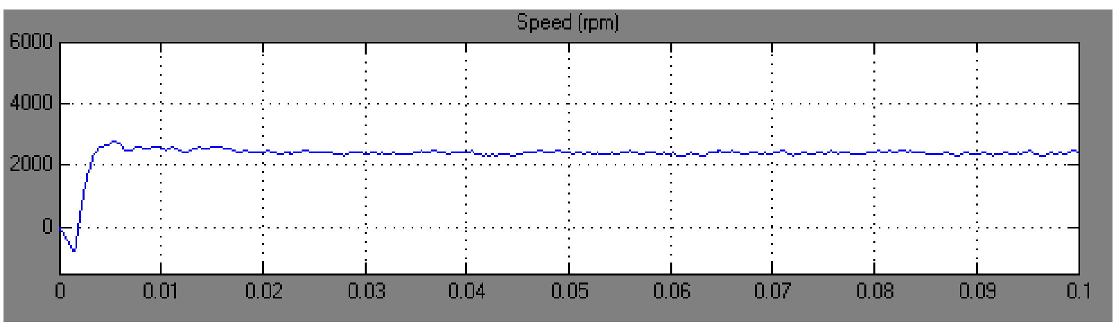

Figure 25. Electrical Speed with time (at 80 Hz); for Hysteresis controller

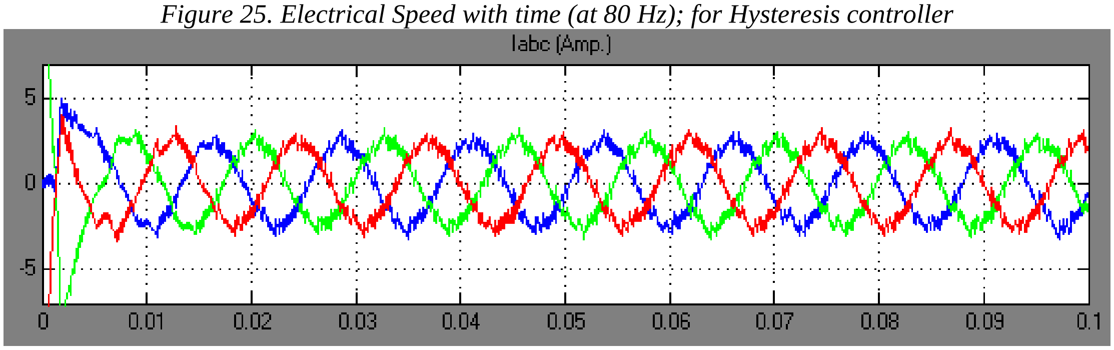

Figure 26. Iabc with time (at 80 Hz); for Hysteresis controller

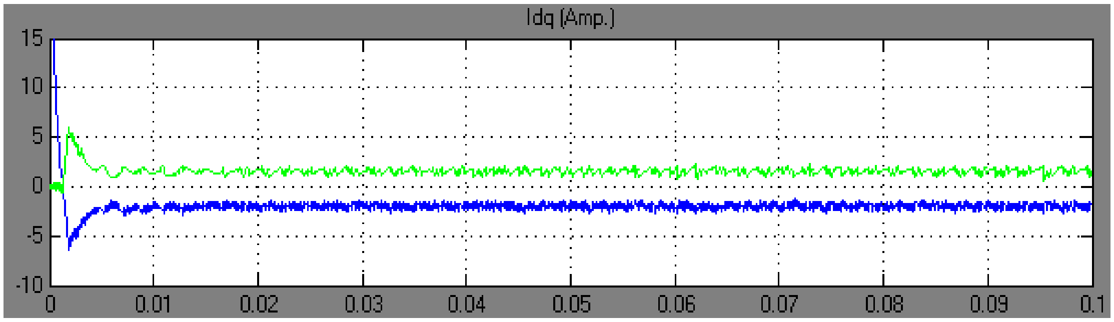

Figure 27. Idq with time (at 80 Hz); for Hysteresis controller

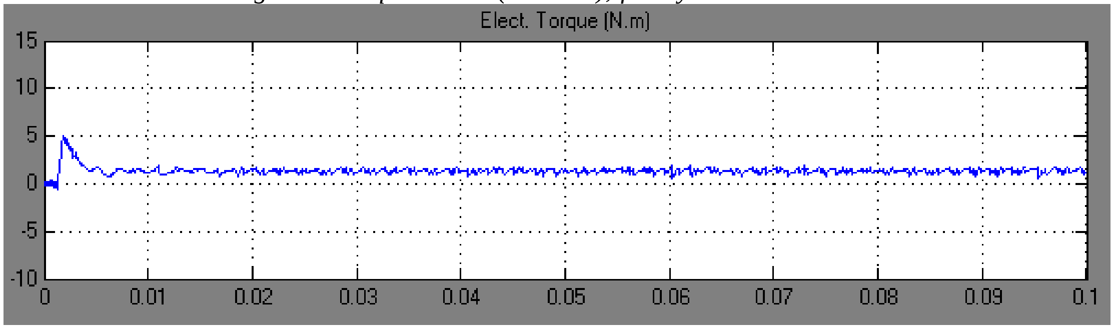

Figure 28. Torque with time (at 80 Hz); for Hysteresis controller

Fig. 25 shows a variation of the speed with time. The steady state speed is the same as that of the commanded reference speed. Fig. 26 shows the three phase currents as a result of the hysteresis current control obtained from Park's reverse transformation. It is clear that the current is non sinusoidal at the starting and becomes sinusoidal when the motor reaches the controller command speed. The corresponding dq component of current is given in fig. 27. Both d and q axis current are present. However the q axis current is small since the torque gets reduced at higher speed, operating at constant power region. Fig. 28 shows the developed torque of the motor with high starting torque.

The above plots have been repeated with PWM control for comparing with hysteresis control.

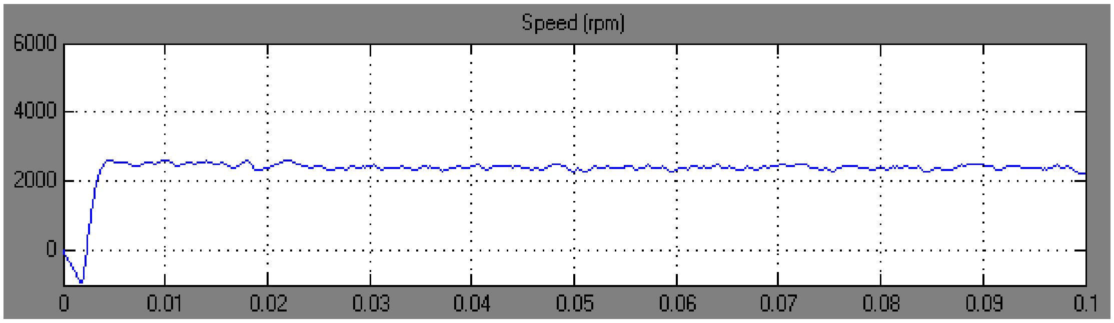

Figure 29. Electrical Speed with time (at 80 Hz); for PWM controller

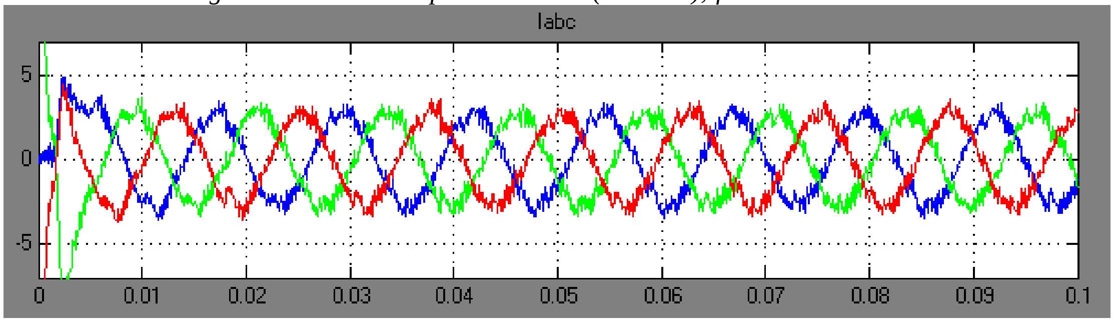

Figure 30. Iabc with time (at 80 Hz); for PWM controller

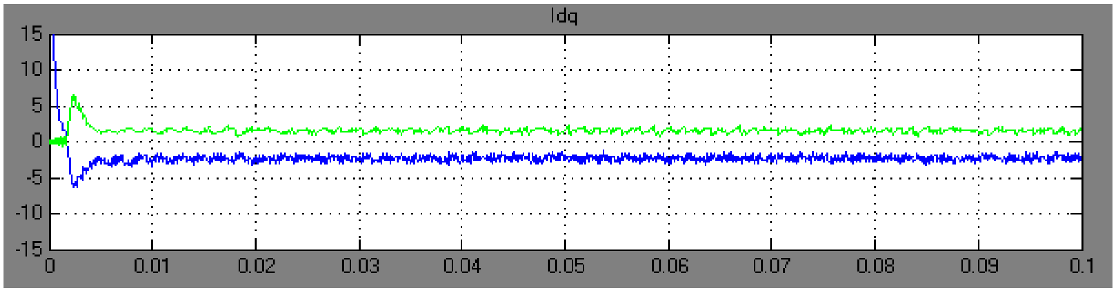

Figure 31. Idq with time (at 80 Hz); for PWM controller

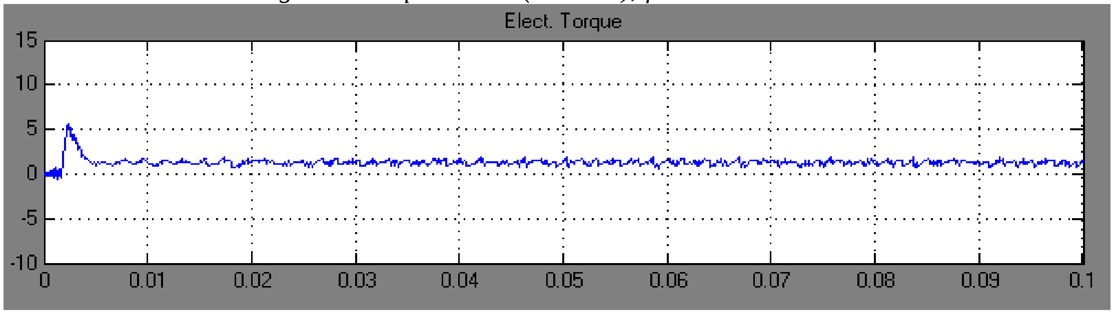

Figure 32. Torque with time (at 80 Hz); for PWM controller

Fig. 29 shows a variation of the speed with time. The steady state speed is the same as that of the commanded reference speed. Fig. 30 shows the three phase currents as a result of the PWM current control obtained from Park's reverse transformation. It is clear that the current is non sinusoidal at the starting and becomes sinusoidal when the motor reaches the controller command speed at steady state. The corresponding dq component of current is given in fig. 31. Both d and q axis current are present. However the q axis current is small since the torque gets reduced at this higher speed due to power being maintained constant. Fig. 32 shows the developed torque of the motor.

5. CONCLUSIONS

A detailed Simulink model for a PMSM drive system with field oriented control has being developed and operation at and above rated speed has been studied using two current control schemes. Simulink has been chosen from several simulation tools because its flexibility in working with analog and digital devices. In the present simulation measurement of currents and voltages in each part of the system is possible, thus permitting the calculation of instantaneous or average losses, and efficiency. Usually in such a drive system the inverter is driven either by hysteresis or by PWM current controllers. A comparative study has been made of the two current control schemes. A speed controller has been designed successfully for closed loop operation of the PMSM drive system so that the motor runs at the commanded or reference speed.

6. REFERENCES

[1] B. K. Bose, “Power electronics and motion control-Technology status and recent trends,” IEEE Trans. Ind. Applicat., vol. 29, pp. 902–909, Sept. /Oct., 1993.
[2] W. Leonhard, “Adjustable speed ac drives,” Proceedings of IEEE, vol. 76, pp. 455-471, April, 1988.
[3] B. K. Bose, “Variable frequency drives-technology and applications,” in Proc. ISIE 93(Budapest), June, 1993, pp 1-18.
[4] R. Gabriel, W. Leonhard, and C. Nordby, “Field oriented control of standard AC motor using microprocessor,” IEEE Trans. Ind. Applicat., vol. IA-16, pp. 186–192, 1980.
[5] L. Harnefors, “Design and analysis of general rotor-flux oriented vector control systems,” IEEE Trans. Ind. Electron., vol. 48, pp. 383–389, Apr. 2001.
[6] M. Schroedl, “Sensorless control of AC machines at low speed and standstill based on the “INFORM” method,” in Conf. Rec. IEEE-IAS Annu. Meeting, vol. 1, 1996, pp. 270–277.
[7] P. L. Jansen and R. D. Lorentz, “Transducerless position and velocity estimation in induction and salient AC machines,” IEEE Trans. Ind. Applicat., vol. 31, pp. 240–247, Mar./Apr. 1995.
[8] P. L. Jansen, R. D. Lorenz, and D. W. Novotny, “Observer-based direct field orientation: Analysis and comparison of alternative methods,” IEEE Trans. Ind. Applicat., vol. 30, pp. 945–953, July/Aug. 1994.
[9] T. M. Jahns and V. Blasko, “Recent advances in power electronics technology for industrial and traction machine drives,” Proc. IEEE, vol. 89, pp. 963–975, June 2001.

[10] Thomas M. Jahns, "Motion control with permanent-magnet ac machines," in Proc. IEEE, vol. 82, Aug. 1994, pp. 1241-12

[11] El Shewy, H and, El Shahat, A, "PM Synchronous Machine Stabilization Control for Electric Vehicle", Ref: 118, Accepted in The Third Ain Shams University International Conference on Environmental Engineering (Ascee-3), April 14-16 2009, Cairo, Egypt.

[12] A. Emadi, S. S. Williamson, and A. Khaligh, "Power electronics intensive solutions for advanced electric, hybrid electric, and fuel cell vehicular power systems", IEEE Trans. Power Electron., vol. 21, no. 3, pp. 567-577, May 2006.

[13] W. Cai, "Comparison and review of electric machines for integrated starter alternator applications", Conf. Rec. IEEE 39th IAS Annu. Meeting, vol. 1, 2004, pp. 386-393.

[14] J. R. Hendershot and T. J. E. Miller, Design of Brushless Permanent Magnet Motors, Oxford, U.K.: Magna Physics Publishing and Clarendon Press, 1994.

[15] M. Zeraoulia, "Electric motor drive selection issues for HEV propulsion systems: A comparative study," IEEE Trans. Vehicular Tech., vol. 55, pp.1756-1763, Nov. 2006.

[16] H. El Shewy, A. El Shahat, "PM Synchronous Machine Stabilization Control for Electric Vehicle", Paper Ref.: 911, Accepted in Global Conference on Renewable and Energy Efficiency for Desert Regions (GCREEDER2009), Amman, Jordan.

[17] B. K. Bose, Power Electronics and Variable Frequency Drives, 1 ed: Wiley, John & Sons, 1996.

[18] P. Pillay and R. Krishnan, "Modeling, simulation, and analysis of permanent-magnet motor drives. I. The permanent-magnet synchronous motor drive," Industry Applications, IEEE Transactions on, vol. 25, pp. 265-273, 1989.

[19] R. Krishnan, Electric Motor Drives Modeling, Analysis, and Control, Pearson Education, 2001.

[20] X. Junfeng, W. Fengyan, F. Jianghua, and X. Jianping, "Flux-weakening control of permanent magnet synchronous motor with direct torque control consideration variation of parameters," Industrial Electronics Society, IECON 2004. 30th Annual Conference of IEEE, Vol. 2, pp. 1323- 1326, 2004.

[21] A. Munoz-Garcia and D. W. Novotny, "Utilization of Third Harmonic-Induced-Voltages in PM Generators," Industry Applications Conference, 1996. Thirty-First IAS Annual Meeting, IAS apos;96., Vol. 1, 6-10 Oct 1996, Page(s):525 – 532.

[22] Kazmierkowski M.P., Tunia H.: Automatic Control Of Converter-Fed Drives, Elsevier Science & Technology (United Kingdom), 1994

[23] Ned Mohan, Tore M. Undeland and William P. Robbins, Power electronics, Converters, Applications and Design, Third Edition, USA ISBN 0-471-22693-9, John Wiley & Sons, Inc.

[24] Krishnan R.: Electric Motor Drives: Modeling, Analysis & Control, Prentice Hall. 2006.

[25] Adel El Shahat, and Hamed El Shewy, "Permanent Magnet Synchronous Motor Dynamic Modeling" Paper ID: X305, Accepted in 2nd International Conference on Computer and Electrical Engineering (ICCEE 2009); Dubai, UAE, December 28 - 30, 2009.

[26] H. M. El Shewy, F. E. Abd Al Kader, M. El Kholy, and A. El Shahat, " Dynamic Modeling of Permanent Magnet Synchronous Motor Using MATLAB - Simulink" EE108, 6th International Conference on Electrical Engineering ICEENG 2008, 27-29 May, 2008, Military Technical College, Egypt.

[27] Adel El Shahat, Hamed El Shewy, "PM Synchronous Motor Dynamic Modeling with Genetic Algorithm Performance Improvement", International Journal of Engineering, ISSN 2141-2839 (Online); ISSN 2141-2820 (Print); Science and Technology Vol. 2, No. 2, 2010, pp. 93-106.

Biographical notes:

Adel El Shahat is currently a Research Scientist, ECE Dept., Mechatronics-Green Energy Lab, The Ohio State University, USA. His interests are: Electric Machines, Artificial Intelligence, Renewable Energy, Power System, Control Systems, PV cells, Power Electronics, and Smart Grids. He has nearly 60 publications between international Journals papers, refereed conferences papers, book chapters and abstracts or posters. He is a Member of IEEE, IEEE Computer Society, ASEE, IAENG, IACSIT, EES, WASET and ARISE. Also, he is member of editorial team and reviewer for six international journals. He gains honors and recognitions from OSU, USA 2009, Suez Canal University Honor with university Medal in 2006, Merit Ten Top-up Students Award of each Faculty from Arab Republic of Egypt, in 2000, and EES, 1999, Egypt.

Hamed El Shewy currently is a Professor of Electrical Machines in the Electrical Power and Machines Department, Faculty of Engineering, Zagazig University, Zagazig, Egypt. He was the previous head of the same department. His research interests include Electric Machines, Power Systems, Power Electronics, and Electric Drives.